

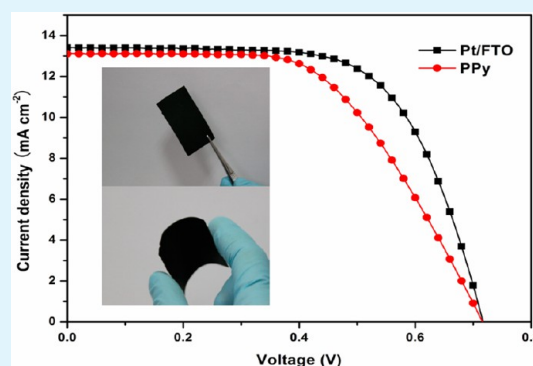
Self-Assembled Free-Standing Polypyrrole Nanotube Membrane as an Efficient FTO- and Pt-Free Counter Electrode for Dye-Sensitized Solar Cells

Tao Peng, Weiwei Sun, Chengliang Huang, Wenjing Yu, Bobby Sebo, Zhigao Dai, Shishang Guo, and Xing-Zhong Zhao*

School of Physics and Technology and Key Laboratory of Artificial Micro- and Nano-Structure of the Ministry of Education, Wuhan University, Wuhan 430072, China

ABSTRACT: The construction of nanoporous conductive polymer membranes has potential applications in catalysts and energy-conversion devices. In this letter, we present a facile method to prepare free-standing polypyrrole (PPy) nanotube films by simply heating pulp-like homogeneous suspensions at a low temperature, which can be employed as a novel counter electrode (CE) to substitute for the expensive fluorine-doped tin oxide (FTO) glass and Pt used in dye-sensitized solar cells (DSSCs). The DSSCs assembled with these paper-like PPy membranes show an impressive conversion efficiency of 5.27%, which is about 84% of the cell with a conventional Pt/FTO CE (6.25%).

KEYWORDS: dye-sensitized solar cells, self-assembled, free-standing, polypyrrole nanotube membrane, counter electrode, FTO- and Pt-free



INTRODUCTION

Dye-sensitized solar cells (DSSCs) have been well-studied since their groundbreaking discovery in 1991 because of their simple preparation process, considerable efficiency for energy conversion, and potential commercial value.¹ The counter electrode (CE) plays an indispensable role in DSSCs by collecting electrons from the external circuit and fulfilling the catalytic reduction of iodide ions.^{2,3} Platinized F-doped SnO₂ (FTO) glass is applied as a counter electrode in DSSCs because of its high conductivity and excellent catalytic property. However, the high cost of Pt and FTO glass limits their large-scale commercialization and application in DSSCs.^{4,5} Moreover, the rigidity of FTO glass restricts the development of a flexible counter electrode and cannot fulfill the demands of flexible solar cells and roll-to-roll fabrication.^{6,7} Therefore, a large amount of research effort has been focused on developing both alternative materials (such as carbonaceous materials, conductive polymers, and sulfides) that have a low cost, high conductivity, and efficient electrochemical catalytic ability to replace Pt^{8–14} and novel substrates such as plastic foils, metals, and graphite paper to fabricate flexible electrodes.⁵

As a functional conductive polymer, polypyrrole (PPy) has attracted much interest as a promising candidate for use as a Pt CE owing to its facile synthesis, good electrical conductivity, high chemical stability, and favorable catalytic efficiency.¹⁵ A PPy CE is usually fabricated by a deposition method or an in situ polymerization method. However, FTO substrates are essential to the method mentioned above; as a result, PPy CE

cannot be used in flexible DSSCs. To save on cost and to fulfill the demand for preparing flexible DSSCs, we prepared for the first time a free-standing paper-like membrane composed of PPy nanotubes that can be used as an efficient FTO- and Pt-free CE. The flexible free-standing membrane has considerable mechanical properties. The efficiency of energy conversion of a DSSC employing the flexible PPy membrane CE can reach as high as 5.27%.

EXPERIMENTAL SECTION

Preparation of PPy Membrane Electrode and Pt Electrode.

The PPy nanotubes were synthesized by a reactive self-degraded template method.¹⁶ About 2.592 g of FeCl₃·6H₂O was added to 320 mL of a 5 mM methyl orange deionized water solution. After stirring for 0.5 h, 0.56 mL of pyrrole monomer was dropped into the mixture followed by stirring for 4 h at about 12 °C. The PPy nanotubes were then obtained after the precipitate was washed several times with deionized water until the filtrate became colorless and neutral.

The PPy nanotubes were doped in 2 M HCl for 12 h and then dispersed in ethanol after being rinsed by deionized water and ethanol. Afterward, the suspension was poured into a glass petri dish. Then, the PPy paper-like membrane was self-assembled from the PPy nanotubes under a vacuum atmosphere at 40 °C for 12 h. Pictures of the PPy membrane are shown in Figure 1.

Received: September 28, 2013

Accepted: December 17, 2013

Published: December 17, 2013

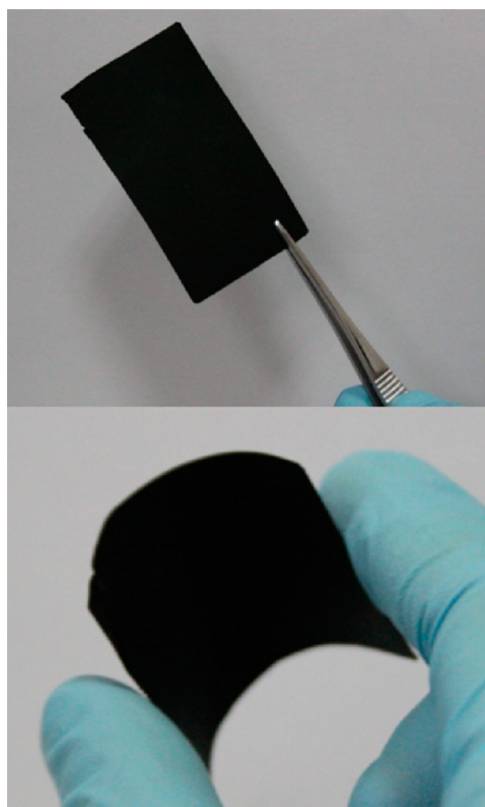


Figure 1. Photographs of the flexible PPy paper-like membrane.

For comparison, Pt/FTO CEs were fabricated by sputtering an ~ 50 nm thick layer of platinum on the FTO glass.

Assembling the DSSCs. Dye-sensitized mesoporous TiO_2 photoanodes were fabricated using a previously reported method.¹⁷ The solution, composed of 0.1 M 1-propyl-3-methylimidazolium iodide (PMII), 0.03M I_2 , 0.05 M LiI, 0.1 M GNCS, and 0.5 M 4-*tert*-butylpyridine (TBP) in a mixed solvent of propylene carbonate (PC) and acetonitrile, was applied as the electrolyte.

Measurement and Characterization. The Raman spectrum was recorded by a Raman microscope (HR800, Horiba). The microstructure of the PPy paper was studied by transmission electron microscopy (JEOL) and scanning electron microscopy (Sirion FEG). The specific surface area of the PPy paper was studied by Brunauer–Emmett–Teller (BET) nitrogen sorption–desorption measurement (LW-BK, China). Photovoltaic measurements of the DSSCs were recorded by applying an external potential bias to the cell with an effective area of 0.25 cm^2 under AM 1.5 simulated illumination (Newport, 91192) with a power density of 100 mW/cm^2 . The electrochemical impedance spectroscopy (EIS) measurements and Tafel polarization measurements were performed on a CHI 660C.

RESULTS AND DISCUSSION

The Raman spectrum of the PPy nanotubes (Figure 2) showed characteristic peaks at 1573 and 1386 cm^{-1} , which represent the backbone stretching mode of the $\text{C}=\text{C}$ bond and the ring stretching mode of PPy, respectively.^{18,19} The bonds around 1048 , 984 , and 917 cm^{-1} are related to the in-plane and out-of-plane vibrations of the $\text{N}-\text{H}$ and $\text{C}-\text{H}$ modes.¹⁹ It can be observed from the TEM image that the flexible PPy membrane is composed of nanotubes that are about 50 nm in diameter (Figure 3a,b). The adequately dispersed PPy nanotube slurry in ethanol forms PPy paper-like membrane when it is restricted in the container under a vacuum atmosphere at a low temperature. In the period of evaporation of ethanol from the PPy nanotube slurry, the nanotubes aggregated to develop into a piece of

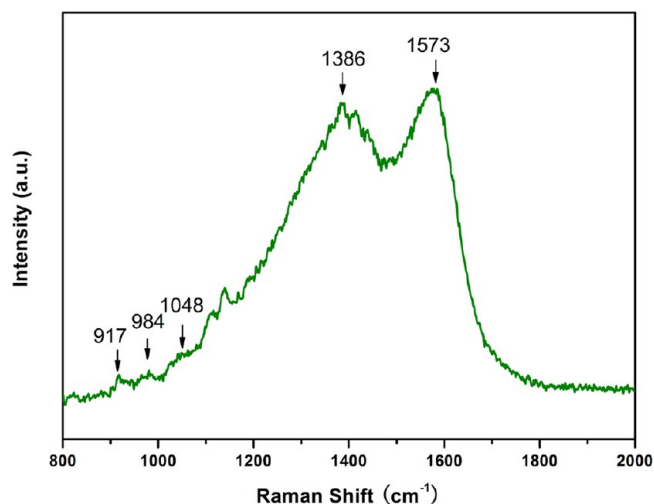


Figure 2. Raman spectrum of the PPy nanotube membrane.

membrane with a uniform thickness. The scanning electron microscope (SEM) image (Figure 4a) shows the tangled PPy nanotubes aggregated to form such a membrane with an open porous network structure that exhibited a larger specific surface area and increased porosity to enhance the catalysis of I_3^- to I^- . The BET nitrogen sorption measurement indicated that the PPy membrane possesses a high surface area of $95 \text{ m}^2/\text{g}$. Figure 4b shows a cross-sectional image of the nanotube membrane with a thickness of about $184 \mu\text{m}$, demonstrating that bundles of PPy nanotubes twined together to form many layers that stacked, constituting the membrane. Thus, the paper-like PPy membrane was prepared via a self-assembly procedure during evaporation. The conductivity and square resistance of the PPy membrane ($\sim 184 \mu\text{m}$ thick) was about 6.6 S/cm and $8.2 \Omega/\text{sq}$, respectively, and the square resistance of Pt/FTO was about $4.5 \Omega/\text{sq}$.

The photovoltaic characteristics of DSSCs employing the flexible PPy membrane and a Pt/FTO CE is shown in Figure 5. Details of the photovoltaic performance parameters are listed in Table 1. The DSSC with a typical Pt/FTO CE had an open-circuit voltage (V_{oc}) of 717 mV , a short-circuit current density (J_{sc}) of 13.41 mAcm^{-2} , a fill factor (FF) of 0.65 , and a conversion efficiency (η) of 6.25% . The parameters of DSSC employing the PPy membrane CE were 716 mV , 13.10 mAcm^{-2} , and 0.56 , respectively. Obviously, the V_{oc} values of the DSSC based on the Pt/FTO and PPy electrodes are almost the same, but the J_{sc} and FF values of the DSSC employing the PPy membrane CE are lower than those of the DSSC based on the Pt/FTO CE. As a result, the overall performance of the DSSC based on the PPy membrane CE is about 84% of that of the cell with a conventional Pt/FTO CE.

To investigate the catalytic activities of electrodes, a Tafel polarization curve test (Figure 6) was carried out on the symmetric cells. The slope for the anodic and cathodic branches in the Tafel zone of the Pt electrode was larger than that of PPy electrode, indicating that the Pt electrode has a higher exchange-current density (J_0) and a superior catalytic activity compared to the PPy electrode.^{8,20}

To study the electrochemical properties of the CEs further, electrochemical impedance spectra (EIS) analysis was carried out. The Nyquist diagrams of symmetric cells are shown in Figure 7. The charge-transfer resistance (R_{ct}) at the electrode/electrolyte interface relates to the intrinsic catalytic properties

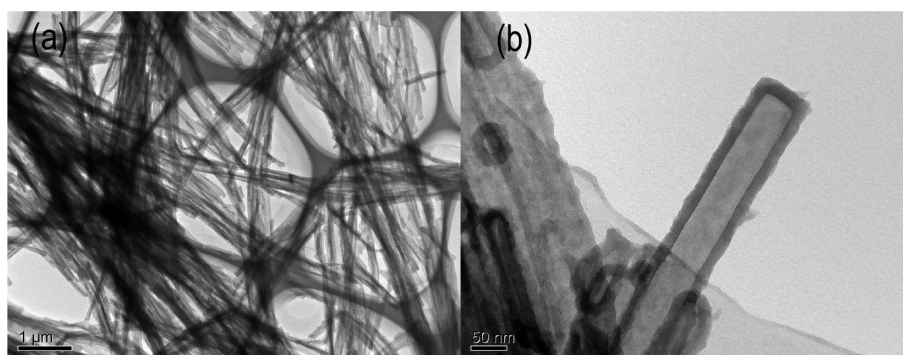


Figure 3. TEM images of PPy tubes.

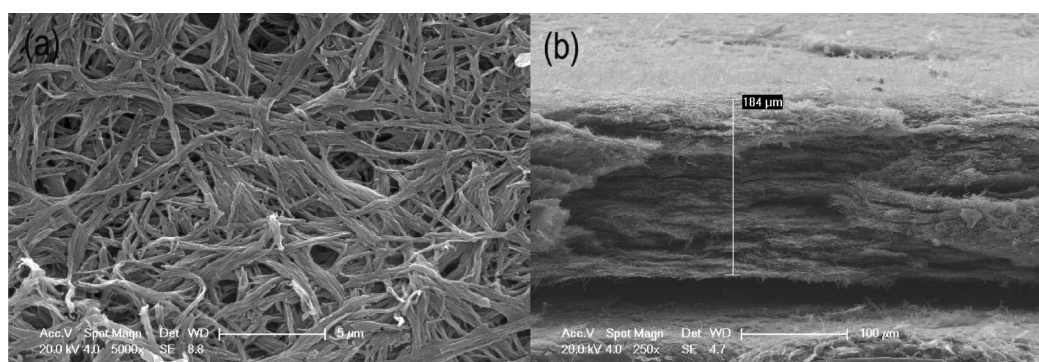


Figure 4. (a) Surface and (b) cross-sectional SEM images of the PPy paper-like membrane.

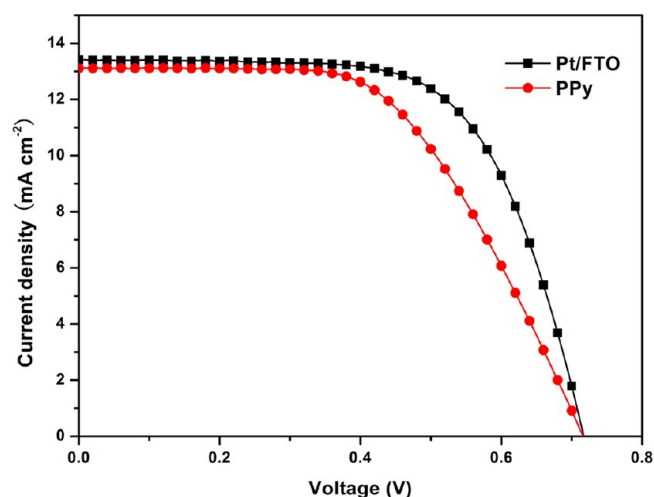


Figure 5. I - V characteristic curves of DSSCs employing Pt/FTO and PPy CEs.

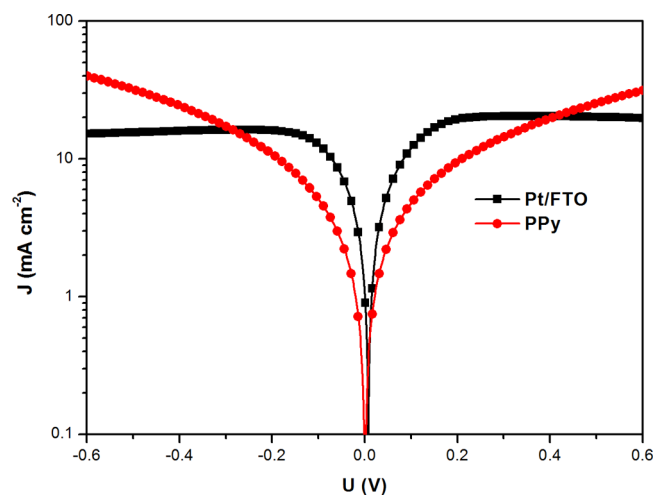


Figure 6. Tafel curves of the symmetrical cells based on two identical Pt/FTO and PPy CEs.

of the counter electrode materials for the reduction of I_3^- to I^- .²¹ Obviously, the R_{ct} of the Pt electrode ($1.71 \Omega \text{ cm}^2$) is lower than that of the PPy electrode ($5.01 \Omega \text{ cm}^2$), which indicates that Pt has a better catalytic activity for I_3^- reduction

than PPy. This result coincided with the exchange current density values according to the following eq 1

$$J_0 = RT/nFR_{ct} \quad (1)$$

Table 1. Photovoltaic Performance Data of DSSCs Employing FTO/Pt and PPy Membrane CEs and EIS Data of the Symmetrical Cells Based on Pt/FTO and PPy CEs

	V_{oc} (mV)	J_{sc} (mA cm^{-2})	FF	efficiency (%)	R_s ($\Omega \text{ cm}^2$)	R_{ct} ($\Omega \text{ cm}^2$)	$C\mu$ (μF)
Pt/FTO	717	13.41	0.65	6.25	0.85	1.71	22.44
PPy	716	13.10	0.56	5.27	8.44	5.01	1679

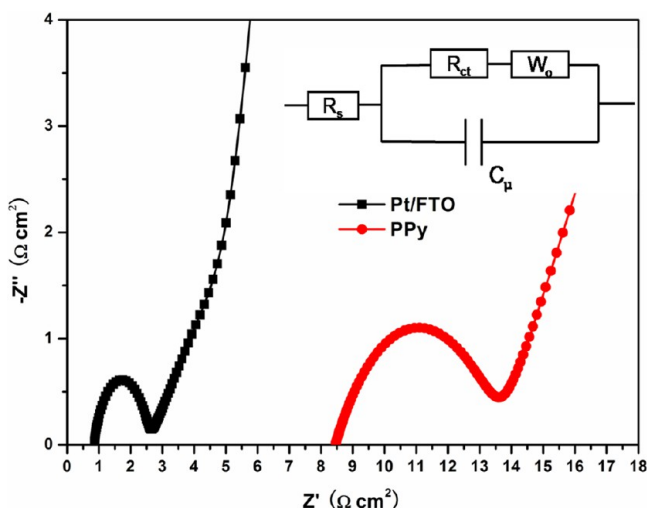


Figure 7. Nyquist diagrams of the symmetrical cells based on two identical Pt/FTO and PPy CEs.

Every factor in this equation has its usual meaning. The double-layer capacitance in the interface between the electrolyte and electrode could be obtained from the EIS, which reflects the active surface area for the electrocatalytic reaction.²⁰ The PPy paper counter electrode had a much higher C_{μ} (1679 μF) compared to that of the Pt electrode (22.44 μF), which can be ascribed to the higher specific surface area (95 m^2/g) and the good electrolyte penetration in the porous PPy membrane and is advantageous for the catalytic performance. As a result, the larger electrocatalytic surface area made up for the relatively poorer intrinsic catalytic properties, so the J_{sc} value of the DSSC based on the PPy membrane CE was close to J_{sc} value of the DSSC based on the Pt/FTO CE. Unfortunately, the series resistance (R_s) of the PPy symmetric cell (8.44 $\Omega \text{ cm}^2$) was higher compared that of the Pt symmetric cell (0.85 $\Omega \text{ cm}^2$), which is attributed to the relatively poor conductivity of PPy and higher square resistance compared with Pt/FTO, yielding a lower FF in this DSSC device.²² As a result, the DSSC assembled with these paper-like PPy membranes has an impressive conversion efficiency of 5.27%, which is about 84% of the cell with a conventional Pt/FTO CE (6.25%).

CONCLUSIONS

A flexible PPy paper-like membrane was obtained by the self-assembly of PPy nanotubes and was used directly as an efficient FTO- and Pt-free counter electrode for a DSSC. The DSSC employing the flexible PPy membrane CE achieved a remarkable conversion efficiency of 5.27%, which matches that of a DSSC with a Pt/FTO CE. Compared to DSSCs based on the typical Pt/FTO CE, the invention of DSSCs employing flexible PPy paper-like membrane CE will benefit the production of low-cost flexible DSSCs, which highlights the extensive use of DSSCs.

AUTHOR INFORMATION

Corresponding Author

*E-mail: xzzhao@whu.edu.cn.

Notes

The authors declare no competing financial interest.

ACKNOWLEDGMENTS

We gratefully acknowledge the financial support from the National Basic Research Program (no. 2011CB933300) of China and the National Science Fund for Talent Training in Basic Science (grant no. J1210061).

REFERENCES

- O'Regan, B.; Grätzel, M. *Nature* **1991**, *353*, 737–740.
- Hou, Y.; Wang, D.; Yang, X. H.; Fang, W. Q.; Zhang, B.; Wang, H. F.; Lu, G. Z.; Hu, P.; Zhao, H. J.; Yang, H. G. *Nat. Commun.* **2013**, *4*, 1583.
- Lin, J.-Y.; Liao, J.-H.; Hung, T.-Y. *Electrochem. Commun.* **2011**, *13*, 977–980.
- Zhou, H.; Shi, Y.; Qin, D.; An, J.; Chu, L.; Wang, C.; Wang, Y.; Guo, W.; Wang, L.; Ma, T. *J. Mater. Chem. A* **2013**, *1*, 3932–3937.
- Sun, H.; Luo, Y.; Zhang, Y.; Li, D.; Yu, Z.; Li, K.; Meng, Q. *J. Phys. Chem. C* **2010**, *114*, 11673–11679.
- Ito, S.; Rothenberger, G.; Liska, P.; Comte, P.; Zakeeruddin, S. M.; Péchy, P.; Nazeeruddin, M. K.; Grätzel, M. *Chem. Commun.* **2006**, 4004–4006.
- Kuang, D.; Brillet, J. r. m.; Chen, P.; Takata, M.; Uchida, S.; Miura, H.; Sumioka, K.; Zakeeruddin, S. M.; Grätzel, M. *ACS Nano* **2008**, *2*, 1113–1116.
- Wang, M.; Anghel, A. M.; Marsan, B.; Cevey, H. N. L.; Pootrakulchote, N.; Zakeeruddin, S. M.; Grätzel, M. *J. Am. Chem. Soc.* **2009**, *131*, 15976–15977.
- Yu, K.; Wen, Z.; Pu, H.; Lu, G.; Bo, Z.; Kim, H.; Qian, Y.; Andrew, E.; Mao, S.; Chen, J. *J. Mater. Chem. A* **2013**, *1*, 188–193.
- Yang, Z.; Liu, M.; Zhang, C.; Tjui, W. W.; Liu, T.; Peng, H. *Angew. Chem., Int. Ed.* **2013**, *52*, 1–5.
- Cai, X.; Hou, S.; Wu, H.; Lv, Z.; Fu, Y.; Wang, D.; Zhang, C.; Kafafy, H.; Chu, Z.; Zou, D. *Phys. Chem. Chem. Phys.* **2012**, *14*, 125–130.
- Hou, S.; Cai, X.; Wu, H.; Lv, Z.; Wang, D.; Fu, Y.; Zou, D. *J. Power Sources* **2012**, *215*, 164–169.
- Hou, S.; Lv, Z.; Wu, H.; Cai, X.; Chu, Z.; Zou, D. *J. Mater. Chem.* **2012**, *22*, 6549–6552.
- Hou, S.; Cai, X.; Wu, H.; Yu, X.; Peng, M.; Yan, K.; Zou, D. *Energy Environ. Sci.* **2013**, *6*, 3356–3362.
- Wu, J.; Li, Q.; Fan, L.; Lan, Z.; Li, P.; Lin, J.; Hao, S. *J. Power Sources* **2008**, *181*, 172–176.
- Yang, X.; Zhu, Z.; Dai, T.; Lu, Y. *Macromol. Rapid Commun.* **2005**, *26*, 1736–1740.
- Ito, S.; Murakami, T. N.; Comte, P.; Liska, P.; Grätzel, C.; Nazeeruddin, M. K.; Grätzel, M. *Thin Solid Films* **2008**, *516*, 4613–4619.
- Chen, F. e.; Shi, G.; Fu, M.; Qu, L.; Hong, X. *Synth. Met.* **2003**, *132*, 125–132.
- Chandra, V.; Kim, K. S. *Chem. Commun.* **2011**, *47*, 3942–3944.
- Wu, M.; Lin, X.; Hagfeldt, A.; Ma, T. *Chem. Commun.* **2011**, *47*, 4535–4537.
- Xu, C.; Li, J.; Wang, X.; Wang, J.; Wan, L.; Li, Y.; Zhang, M.; Shang, X.; Yang, Y. *Mater. Chem. Phys.* **2012**, *132*, 858–864.
- Kung, C. W.; Chen, H. W.; Lin, C. Y.; Huang, K. C.; Vittal, R.; Ho, K. C. *ACS Nano* **2012**, *6*, 7016–7025.